Ca^{2+}-dependent K^+ channels from rat olfactory cilia characterized in planar lipid bilayers

Karen Castillo[a,b], Juan Bacigalupo[a,b], Daniel Wolff[a,*]

[a] *Department of Biology, Faculty of Sciences, University of Chile, P.O. Box 653, Santiago, Chile*
[b] *Millennium Institute for Advanced Studies in Cell Biology and Biotechnology, University of Chile, P.O. Box 653, Santiago, Chile*

Abstract **Olfactory cilia contain cyclic nucleotide-gated and Ca^{2+}-dependent Cl^- conductances that underlie excitatory chemotransduction, and a Ca^{2+}-dependent K^+ (K_{Ca}) conductance, apparently involved in inhibitory transduction. Previous single-channel patch-clamp studies on olfactory cilia revealed four different K_{Ca}s, with different conductances and kinetics. Here, we further characterized these channels in planar bilayers, where blockers could be properly tested. All four ciliary K_{Ca}s were observed: The 16 pS channel, $K_{0.5,Ca}$ = 40 μM and apamin-sensitive; the 30 and 50 pS channel, $K_{0.5,Ca}$ = 59 μM, clotrimazole-sensitive and charybdotoxin-insensitive; the 60 pS channel, clotrimazole-sensitive and charybdotoxin-insensitive; and the 210 pS channel, $K_{0.5,Ca}$ = 63 μM, blocked by charybdotoxin and iberiotoxin. The presence of the 16 and 210 pS channels was confirmed by immunoblotting.**

Keywords: Odor transduction; Olfactory cilia; Calcium-activated potassium channel; Lipid bilayer

1. Introduction

Olfactory receptor neurons (ORNs) have a conspicuous morphology, which is conserved across most vertebrate species. Their cell bodies project a thin, unmyelinated axon to the olfactory bulb and a single dendrite that reaches the mucosal epithelial surface, where it swells to form the dendritic knob. From the knob emanate a number of cilia, the organelles where transduction takes place. Indeed, all molecular components involved in transduction reside in the cilia. Three ionic conductances have been found in the ciliary membrane: a cyclic nucleotide-gated (CNG) conductance [1], a Ca^{2+}-dependent Cl^- (Cl_{Ca}) conductance [2] and a Ca^{2+}-dependent K^+ (K_{Ca}) conductance [3,4]. Odorants trigger a cAMP cascade that leads to the opening of cationic CNG channels, resulting in a depolarizing current. Calcium enters the cilia through the CNG channel and activates Cl_{Ca} channels, allowing an efflux of Cl^- that further depolarizes the neuron, increasing its discharge rate [5]. In contrast, the K_{Ca} conductance appears to have the opposite effect, which is to hyperpolarize the cell causing a reduction in the firing rate [3].

The CNG channel has been characterized by whole cell and single-channel recordings from the dendritic knob [5]. It has been cloned and expressed in heterologous systems [6,7]. Its unitary conductance ranges from 12 to 55 pS, depending on the species [5], and it is sensitive to Ca^{2+} channel blockers such as l-*cis* Diltiazem and LY83583 [8]. No toxins that block this channel have been reported. The Cl_{Ca} channel, in contrast, is poorly characterized and its primary sequence remains unknown. The channel unitary conductance has been estimated by noise analysis to be in the order of 0.8 pS [9] and it is blocked by niflumic acid, DIDS and SITS [2,10].

In a recent patch-clamp study [4] conducted in membrane patches excised from toad olfactory cilia, four K_{Ca} channel types were identified: a high-conductance channel (BK_{Ca}; 210 pS), two intermediate conductance channels (IK_{Ca}, one channel of 60, and another one of 30 and 60 pS) and a small-conductance channel (SK_{Ca}, 15 pS). The pharmacological profiles of such channels were not investigated, mainly because charybdotoxin (ChTx) and iberiotoxin (IbTx), well-known blockers of BK_{Ca} channels, and apamin, a toxin that blocks some SK_{Ca} channels, exert their effects from the extracellular aspect of the membrane. Macroscopic data had shown that both ChTx and IbTx partially block the odor-induced K_{Ca} current, presumably by affecting the BK_{Ca} conductance [[10]; Madrid et al., unpublished results]. The study of the effects of toxins upon K_{Ca} channels is not possible in membrane patches, because there is no access to their external (extracellular) side, located inside the pipette. Outside-out patches cannot be obtained with the extremely small patch pipettes required to record from the cilia. To overcome this difficulty, we used the planar lipid bilayer technique, where reconstituted channels derived from a ciliary membrane preparation are accessible to pharmacological analysis from both sides of the membrane. In this study, we present results of the biophysical and pharmacological characterization of the K_{Ca} channels from a purified olfactory cilia fraction, incorporated into planar phospholipid bilayers. Our results confirm the presence of small, intermediate and high-conductance K_{Ca} channels in olfactory cilia and support the notion that they might be involved in vertebrate odor-transduction. Also, they would allow to determine the relative contribution of each K_{Ca} channel subtype to net ciliary odor-triggered K_{Ca} inhibitory current.

*Corresponding author. Fax: +56 2 678 7435.
E-mail address: dwolff@uchile.cl (D. Wolff).

2. Materials and methods

2.1. Preparation of a ciliary membrane fraction from rat olfactory neurons

Membranes were obtained using a modification of method described by Washburn and co-workers [11], which involves mechanical rupturing, sonication and purification in sucrose gradients. Adult Sprague–Dawley rats were sacrificed with anaesthesia overdose (pentobarbitone 60 mg/kg) and nasal olfactory epithelia were surgically removed and suspended in saline (solution 1) containing (in mM): 145 NaCl, 5 KCl, 1.6 K_2HPO_4, 2 $MgSO_4$, 7.5 D-glucose, 20 HEPES, pH 7.4, supplemented with a cocktail of protease inhibitors containing aprotinin, leupeptin, pepstatin, benzamidin and PMSF. All steps were carried out at 4 °C. The suspension was gently rocked for 20 min and centrifuged for 10 min at $1500 \times g$. The supernatant recovered and the pellet was resuspended in solution 1 supplemented with 1 mM EDTA (solution 2) and sonicated using a microprobe at low power for 10 s. The tissue was allowed to settle and the supernatant was recovered. The pellet was resuspended in solution 2, sonicated at low power for 30 s and the supernatant recovered. All the supernatants were pooled together and centrifuged at $1500 \times g$ for 10 min. The supernatant was loaded in a discontinuous sucrose gradient formed by a 20% and a 43% sucrose layers and centrifuged at $100\,000 \times g$ for 1 h. The band in the gradient interface was extracted, diluted 10-fold and centrifuged at $100\,000 \times g$ for 1 h. The pellet containing the cilia was resuspended in solution 1 supplemented with 2 mM EGTA and 0.5 mM sucrose, aliquoted and stored at −70 °C. Protein content was determined with the method of Hartree [12].

2.2. Western blot analysis

Purified olfactory cilia membranes were separated in 8% SDS–PAGE gels, electrotransferred (Mini-*Trans* Blot System; Bio-Rad, Hercules, CA) to nitrocellulose membranes (Hybond ECL; Amersham-Pharmacia, Piscataway, NJ) at 4 °C and incubated with 5% non-fat milk or 3% BSA in Tris-buffered saline (TBS) with 0.05% Tween 20 (TBS-T) for 1 h at room temperature, to block unspecific sites. Membranes were then incubated 2 h at room temperature, or overnight at 4 °C, with the particular antibody: a polyclonal anti-BK_{Ca} channel recognizing a C-terminus intracellular epitope present in vertebrate BK_{Ca} channels (Alomone Labs, Jerusalem, Israel), a polyclonal anti-SK_{Ca} channel recognizing an intracellular N-terminus sequence present in mammals (Alomone Labs, Jerusalem, Israel), a monoclonal anti-voltage-dependent Na^+ channel recognizing an intracellular III–IV loop sequence present in vertebrate Na^+ channels (Sigma–Aldrich, St. Louis, MO), anti CNG channel recognizing an intracellular C-terminus sequence, present in mammals (Alomone Labs, Jerusalem, Israel) or a polyclonal anti-adenylyl cyclase III raised against a peptide mapping at the carboxy-terminus of rat origin adenylyl cyclase III (ACIII, Santa Cruz Biotechnology, Santa Cruz, CA). The membranes were then developed with a chemiluminescence assay (ECL Lumigen PS-3 Detection Reagent; Amersham-Pharmacia, Piscataway, NJ) using horseradish peroxidase-conjugated with the corresponding secondary antibody (anti rabbit for BK_{Ca}, SK_{Ca} and CNG channels, and anti-mouse for Na^+ channel and ACIII).

2.3. Single-channel recording in planar phospholipid bilayers

Bilayers were formed by applying a drop of palmitoyl-oleoyl phosphatidylethanolamine (POPE) or a mixture of POPE and palmitoyl-oleoyl phosphatidylcholine (POPC) 4:1 (Avanti Polar Lipids, Birmingham, AL) dissolved in *n*-decane (20 mg/ml), to a 200 μm diameter hole in a teflon cup separating two saline compartments. Channel insertion occurred spontaneously after touching the bilayer with a droplet of highly purified ciliary membranes. Incorporation of single ionic channels was indicated by the occurrence of discrete current fluctuations as a constant voltage difference was applied across the bilayer. After the incorporation of a channel, single K_{Ca} channel currents were recorded for a few minutes (control) in symmetric 100 mM KCl or K-Acetate (KAc), or 100/20 mM KAc, 5 mM HEPES-K^+, pH 7.0. Free Ca^{2+} concentration in the solution was set at the desired values using variable amounts of $CaCl_2$ and EGTA. Free Ca^{2+} concentrations were calculated with the WinMAXC v2.05 computer program. Single-channel currents were recorded with an 8900 Dagan patch-clamp amplifier (Dagan Corp, Minneapolis, MN). Voltage pulses were applied to the *cis* compartment and the current was recorded from the *trans* side, through Ag/AgCl electrodes connected to the saline compartments with 1 M KCl agar bridges [13]. The current was monitored by an oscilloscope, amplified, digitized (VR-10 PCM, Instrutech Corp, NY) and stored in videotape or in the HDD of a PC, interfaced by a LabMaster data acquisition board (Scientific Solutions, Solon, OH) and analyzed with the pClamp 6 software (Axon Instruments, Union City, CA). Experiments were carried out at room temperature (20 ± 2 °C). Chemicals were purchased from Sigma Chemical (St. Louis, MO) and Merck (Darmstadt, Germany), unless otherwise indicated.

Toxin stock solutions were prepared by dissolving the lyophilized compounds (Alomone Labs, Jerusalem, Israel), in bidistilled water at the following final concentrations: apamin 100 μM, IbTx and ChTX 10 μM, aliquoted and stored at −20 °C until used. Clotrimazole (Sigma Chemical, St. Louis, MO) was dissolved in DMSO. Vehicle (water or DMSO) addition controls were carried out. Calcium and toxins were added to the solution facing the intracellular side and extracellular side of the channel, respectively. K_{Ca} channel orientation in the bilayer was determined by applying voltage pulses of opposite polarity or by checking from which side of the chamber Ca^{2+} increases channel activity.

3. Results

3.1. Purity of the olfactory cilia membrane fraction

To carry out our study of the ciliary K^+ channels in planar lipid bilayers, it was crucial to obtain a highly purified olfactory cilia membrane preparation. The degree of enrichment and purity of the preparation in ciliary membranes was assessed by the Western blot method. The enrichment was tested with antibodies against the ACIII and the CNG channel, membrane proteins that specifically localize to these organelles. The anti-ACIII antibody strongly labelled band in the ciliary and whole cell epithelium fractions, but these bands were less intense in deciliated olfactory epithelium and olfactory bulb, and were not observed in the brain fraction, used as negative control (Fig. 1A). A band in the ciliary fraction was strongly reactive to the anti-CNG channel antibody, being ab-

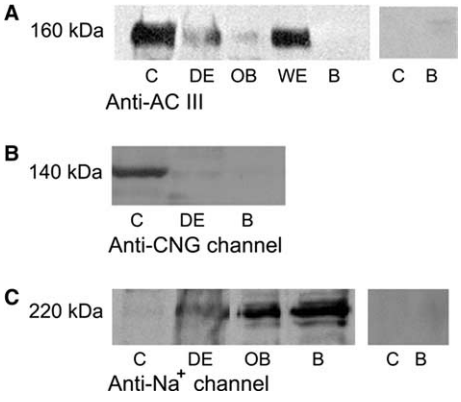

Fig. 1. Enrichment and purity of the ciliary membrane fraction. (A) Western blots of olfactory cilia (C), deciliated olfactory epithelium (DE), olfactory bulb (OB), whole olfactory epithelium (WE) and brain (B) membrane fractions labelled with anti-ACIII (1:1000) antibodies. Brain membranes were used as negative control. The tracks on the right-hand side correspond to the controls without the primary antibodies. (B) Western blots of olfactory cilia, deciliated olfactory epithelium and brain membranes (negative control) labelled with anti-CNG channel antibody (1:600). (C) Western blots of olfactory cilia, deciliated olfactory epithelium, olfactory bulb, and brain (positive control) fractions labelled with anti-voltage-dependent Na^+ channel antibodies (1:300). The controls without primary antibodies are shown in the Western blot at the right in A and C. All lanes (A–C) were loaded with 50 μg protein.

sent in the deciliated epithelium and brain fractions (Fig. 1B). To test for purity of the ciliary membrane fraction with other membranes, we used an antibody against the voltage-dependent Na^+ channel, since this membrane protein is present in the cell body and dendrite, but is not expected to be found in the cilia. Accordingly, the antibody did not label the ciliary fraction, but it reacted with the deciliated epithelium and a brain fraction used as positive control (Fig. 1C).

3.2. Single-channel recordings

Fusion of purified olfactory ciliary membranes to planar lipid bilayers induced the incorporation of several K_{Ca} channels of small, intermediate and high conductance.

3.3. Small conductance Ca^{2+}-dependent K^+ (SK_{Ca}) channels

The open probability (P_0) of this channel was not appreciably affected by voltage, but it was dependent on Ca^{2+} concentration. Fig. 2A illustrates representative unitary currents of a SK_{Ca} channel from the purified ciliary fraction recorded at 60 mV in symmetrical 100 mM KAc and at different free Ca^{2+} concentrations. The channel remained almost silent at 5 μM Ca^{2+}, but its P_0 increased to 0.3 upon elevating free calcium to 20 μM, approaching a maximum value of ~0.6 at 80 μM Ca^{2+}. The P_0 versus Ca^{2+} concentration curve obtained with the data of four experiments, determined a $K_{0.5}$ of 39.8 μM (Fig. 2B). From the *I–V* relations, a slope conductance of 16.3 ± 0.7 pS (mean ± S.E.M., $n = 6$) was determined for this channel (Fig. 2C). To pharmacologically characterize this SK_{Ca} channel, we tested the effect of apamin, a bee toxin that blocks SK3, a subfamily of SK_{Ca} channels [14]. As illustrated in Fig. 2D, the channel is greatly blocked by 22 nM apamin.

To further assess the presence of the SK_{Ca} channel in the rat olfactory cilia fraction, we carried out a Western blot analysis using a polyclonal antibody against the SK3 channel. A single band reacted with the antibody in the ciliary membrane fraction (Fig. 2E) indicating the presence of this SK_{Ca} channel subtype in the cilia. The band was also present in the deciliated epithelia and olfactory bulb fractions. Since this SK_{Ca} channel is differentially expressed in denervated and normal skeletal muscle [15], we used membrane fractions from each muscle condition as positive and negative controls, respectively. As expected, the denervated muscle lane exhibited a reactive band corresponding to SK_{Ca}.

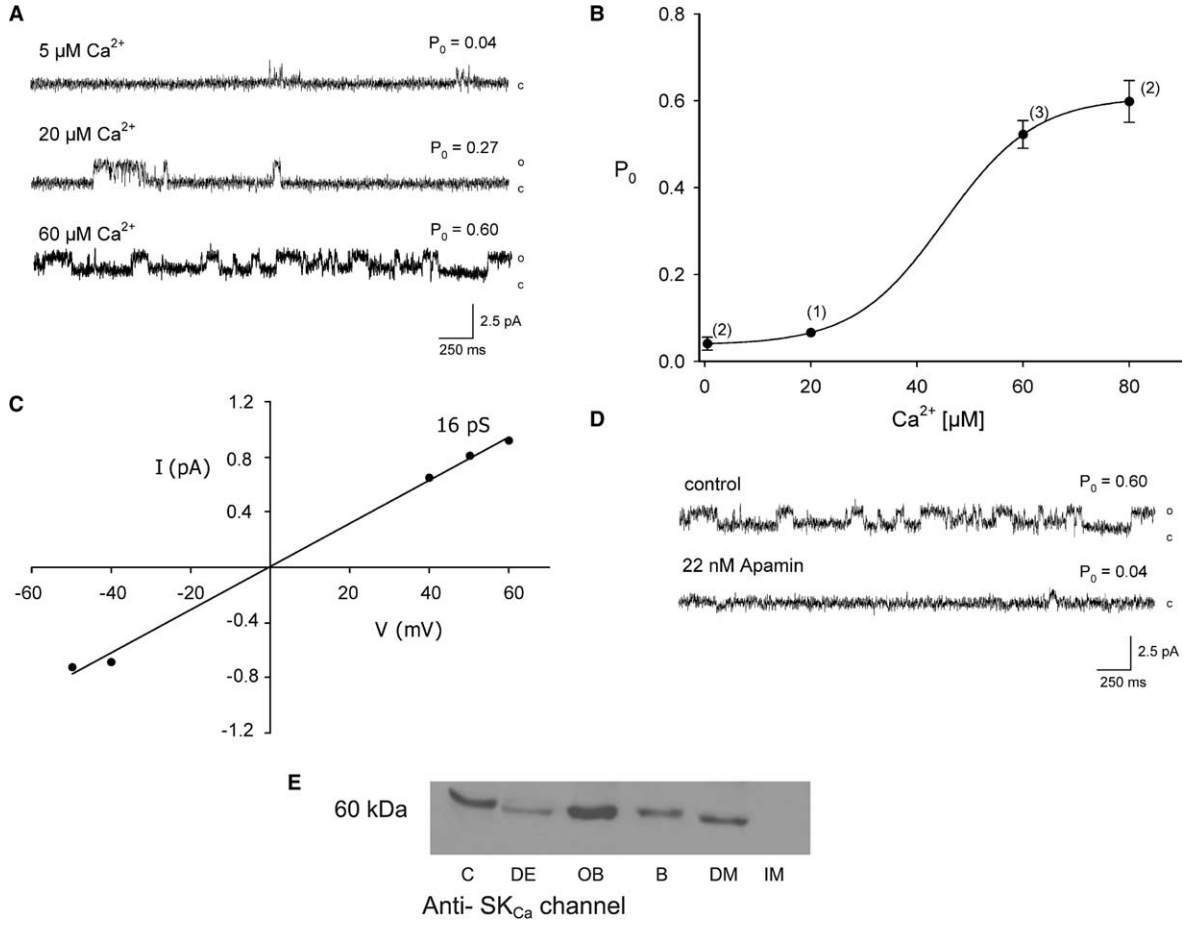

Fig. 2. SK_{Ca} channel. (A) SK_{Ca} channel unitary currents records at three different Ca^{2+} concentrations at +60 mV in symmetrical 100 mM KAc. (B) P_0 versus Ca^{2+} concentration plot for the SK_{Ca} channel at +60 mV. Experimental points were fitted to a Hill equation, with $K_{0.5}$ = 39.8 μM and $n = 3.2$; (C) Representative *I–V* curve, determining a 16 pS slope conductance. (D) SK_{Ca} channel activity was inhibited by 22 nM apamin. Single-channel currents recorded in symmetrical 100 mM KAc, 50 μM Ca^{2+}, at +60 mV. (E) Detection of the SK3 channel in a purified ciliary fraction by Western blotting. The anti-SK3 antibody was used at a 1:600 dilution. Denervated (DM) and innervated (IM) rat skeletal muscle fractions were used as positive and negative controls, respectively. All lanes were loaded with 50 μg protein.

3.4. Intermediate conductance Ca^{2+}-dependent K^+ (IK_{Ca}) channels

In our bilayer study, we identified two K_{Ca} channels with conductances in the intermediate range, referred to as IK_{Ca}-1 and IK_{Ca}-2.

3.5. The IK_{Ca}-1 channel

This channel was voltage independent (not shown) and its open probability increased with Ca^{2+} concentration. Fig. 3A shows unitary current recordings at +50 mV and at two different Ca^{2+} concentrations, in symmetrical 100 mM KAc. A $K_{0.5}$ of 59.5 μM was determined from the P_0 versus Ca^{2+} concentration curve (Fig. 3B). This channel presented two conductance states, as observed at an expanded timescale in Fig. 3C. The corresponding *I–V* relations (Fig. 3D) determine slope conductance values of 30.3 ± 1.4 and 50.5 ± 1.9 pS ($n = 7$), respectively.

This channel was not affected by charybdotoxin (25 nM), but it was blocked by clotrimazole (Fig. 3E). Before addition of the blocker, the channel presented two mean closed times (τ_c) of 6 and 26 ms. After clotrimazole addition at 2.5 μM, the channel presented two τ_c values of 6 and 37 ms and a third τ_c of 6.3 s, attributed to blockade, appeared. Clotrimazole at 6 μM completely blocked the channel.

3.6. The IK_{Ca}-2 channel

This K_{Ca} channel showed a slope conductance of 59.6 ± 1.4 pS ($n = 8$), similar to one of the open states of the IK_{Ca}-1 channel, although it displayed a different kinetics. A representative *I–V* curve is shown in Fig. 4B. Fig. 4A illustrates two current traces 0 and 40 mV, in 100/20 mM KAc, 50 μM Ca^{2+}. This channel was completely blocked by 1 μM clotrimazole (Fig. 4C), but was unaffected by 6 nM ChTx (not shown).

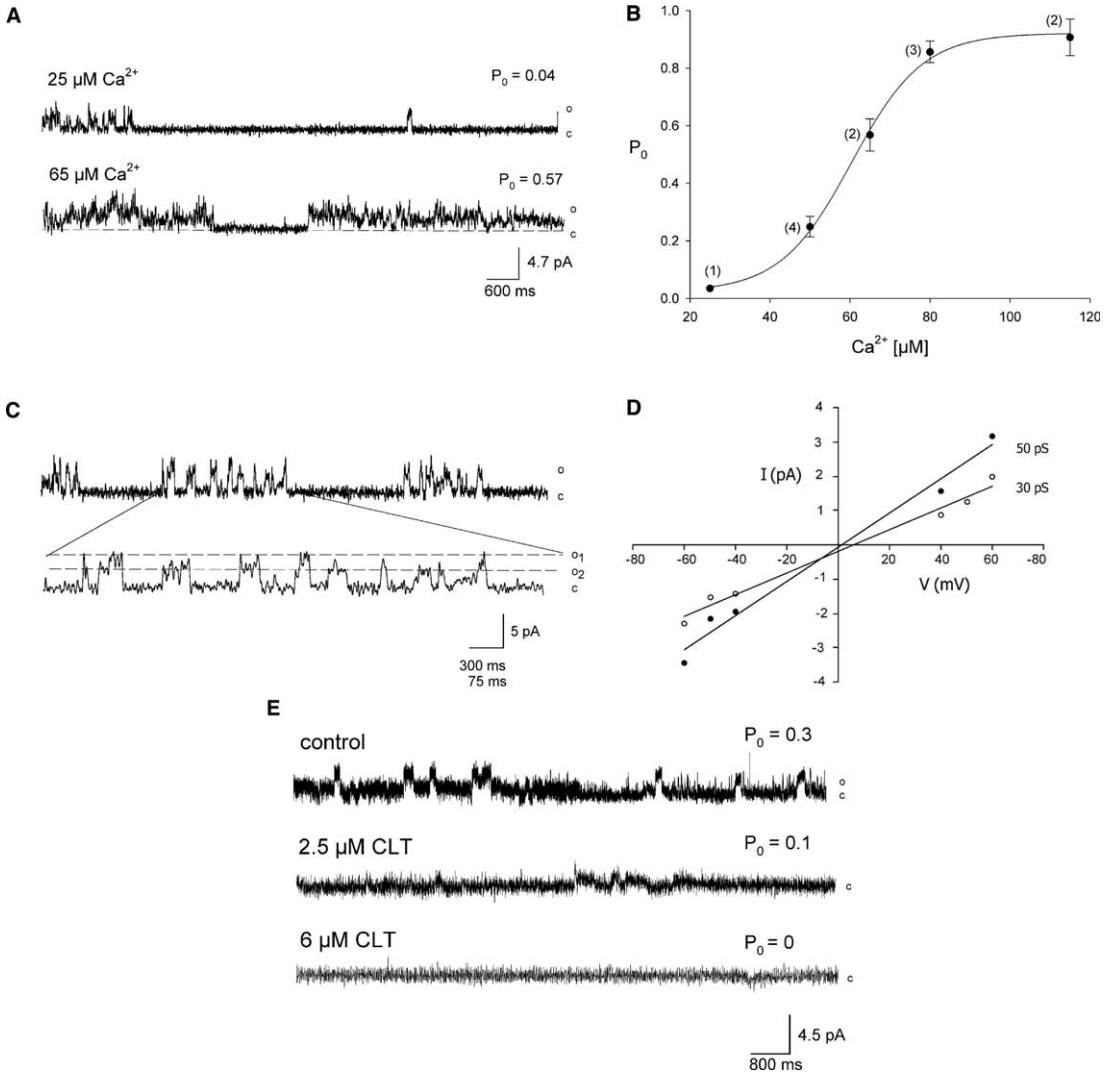

Fig. 3. IK_{Ca}-1 channel. (A) Single-channel current recordings of the IK_{Ca}-1 channel at two different Ca^{2+} concentrations, in symmetrical 100 mM KAc, at +50 mV. (B) P_0 versus [Ca^{2+}] plot for this channel at +50 mV. Experimental points were fitted to a Hill equation, with $K_{0.5} = 59.5$ μM and $n = 6.6$. (C) Single-channel currents recorded at +50 mV and 65 μM Ca^{2+}, presented in an expanded timescale to allow visualization of the two open state levels. (D) Representative *I–V* curve, determining slope conductances of 30 and 50 pS. (E) Effect of clotrimazole on the IK_{Ca}-1 channel activity at 50 μM Ca^{2+} and +60 mV.

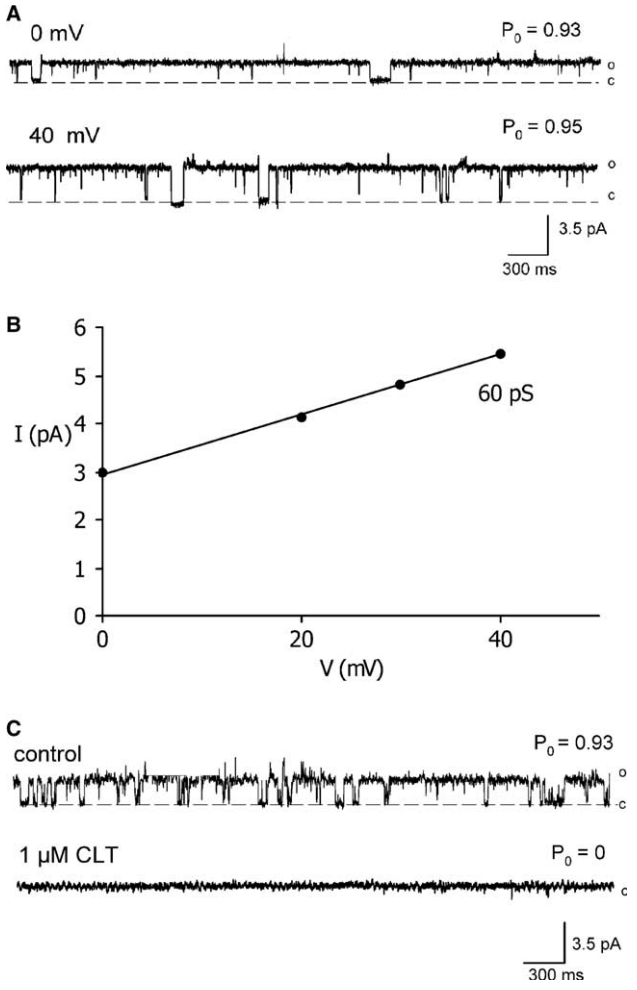

Fig. 4. IK_{Ca}-2 channel. (A) Unitary current recordings of a IK_{Ca}-2 channel at 0 and +40 mV in asymmetrical 100/20 mM KAc solutions and 20 μM Ca^{2+}. (B) Representative *I–V* curve, determining a 60 pS slope conductance. (C) Effect of 1 μM clotrimazole on the channel at 50 μM Ca^{2+}.

3.7. The high-conductance Ca^{2+}-dependent K^+ channel (BK_{Ca})

This was the K^+ channel that most frequently incorporated into bilayers and showed the typical biophysical and pharmacological characteristics of BK_{Ca} channels from other tissues [14]. Fig. 5A offers unitary current recordings of a BK_{Ca} channel in symmetrical 100 mM KAc, 50 μM Ca^{2+} and at three different potentials. Channel P_0 showed pronounced voltage-dependence. Its *I–V* relationship yielded a slope conductance of 210.4 ± 5.8 pS (Fig. 5B; $n = 12$). The Ca^{2+} dependence of this ciliary BK_{Ca} channel is illustrated in Fig. 5C, where traces of channel activity at 40 mV and at three different Ca^{2+} concentrations are presented. Fig. 5D displays the channel P_0 as a function of [Ca^{2+}]. The curve shows the characteristic sigmoidal shape, approaching a P_0 of 1 above 100 μM Ca^{2+} and determines a $K_{0.5}$ of 63.2 μM. This channel was blocked by IbTx, a specific inhibitor of BK_{Ca} channels, and of ChTx, blocker of BK_{Ca} and other voltage-dependent K^+ channels. The sensitivities to these toxins varied widely among the BK_{Ca} channels studied, although the concentrations that completely blocked the channel were in the nanomolar range for both toxins. Fig. 5E shows the effects of IbTx on the BK_{Ca} channel. It can be appreciated that the toxin induced long lasting closed states that increased in duration and frequency as a function of its concentration. Prior to toxin addition the channel presented two mean closed times (τ_c) of 3.0 and 120 ms. After the addition of 44 nM IbTx, the channel presented two τ_c values of 3.0 and 180 ms and a third long τ_c of 3.5 s, corresponding to the blocked state, appeared. IbTx at 110 nM completely blocked the channel. In a few cases, BK_{Ca} channels exhibited a particularly high sensitivity to IbTx, being completely blocked by 4 nM toxin, in contrast with the 110 nM IbTx needed to block the channel in Fig. 5E. This BK_{Ca} channel was also sensitive to ChTx. As illustrated in Fig. 5F, the addition of 11 nM ChTx induced long lasting closed states. Before toxin addition, this channel presented two τ_c values of 7.0 and 24 ms. Following toxin application the channel presented two τ_c values of 6.0 and 25 ms and a third mean closed time of 518 ms, ascribed to the blocked state, appeared.

The presence of BK_{Ca} channels in the olfactory cilia fraction was also examined by Western blotting, using a polyclonal anti-BK_{Ca} channel antibody. Fig. 5G shows a band near 116 kDa that reacted with the antibody, confirming the presence of the channel in the olfactory cilia indicated by the electrophysiological data. This finding is also consistent with previous results from our laboratory, where the presence of the BK_{Ca} channel in the cilia was demonstrated with immunocytochemistry and Western blotting [4]. As expected, the protein was also found in the deciliated epithelia and brain fractions, used as positive controls. The extra bands in both ciliary and brain fractions of the immunoblot, may correspond either to degradation sub-products or to splice variants of the channel.

4. Discussion

Previous electrophysiological studies documented that odorants induce inhibitory responses in isolated vertebrate olfactory neurons, consisting of decreases in the spiking rate [3,5,16,17]. It was also reported that the inhibitory response appears to involve the activation of a ChTx-sensitive, hyperpolarizing K_{Ca} current [10]. This odorant-induced K^+ current was mediated by an increase in cytosolic Ca^{2+} concentration due to an odorant-induced apical Ca^{2+} influx [18]. Evidence from focal odor stimulation experiments on isolated ORNs was consistent with the possibility that this odor-triggered K_{Ca} conductance was present in the cilia [18].

The first single K_{Ca} channel recordings from the soma and dendritic knob of mice ORNs were obtained by Maue and Dionne [19] by means of the patch-clamp technique. The authors identified a 130 pS voltage-dependent K_{Ca} channel with a fast gating kinetics. Later, a planar lipid bilayer study of a toad olfactory ciliary membrane fraction suggested the presence of a 240 pS conductance BK_{Ca} channel (in symmetrical 200 mM KCl). Its $K_{0.5}$ for Ca^{2+} was 46 μM and it was blockable by 42 nM ChTx [20]. This channel was presumably derived from the cilia, although the purity of the membrane fraction was not assessed. In a recent work, Delgado et al. [4] obtained single-channel recordings from inside-out membrane patches excised from toad olfactory cilia. These authors identified four different K_{Ca} channel types, of small (12 pS), intermediate (one of 29 and 60 pS, and another one of 60 pS) and one of large conductance (210 pS), all K^+-selective and sensitive to low micromolar Ca^{2+}. However,

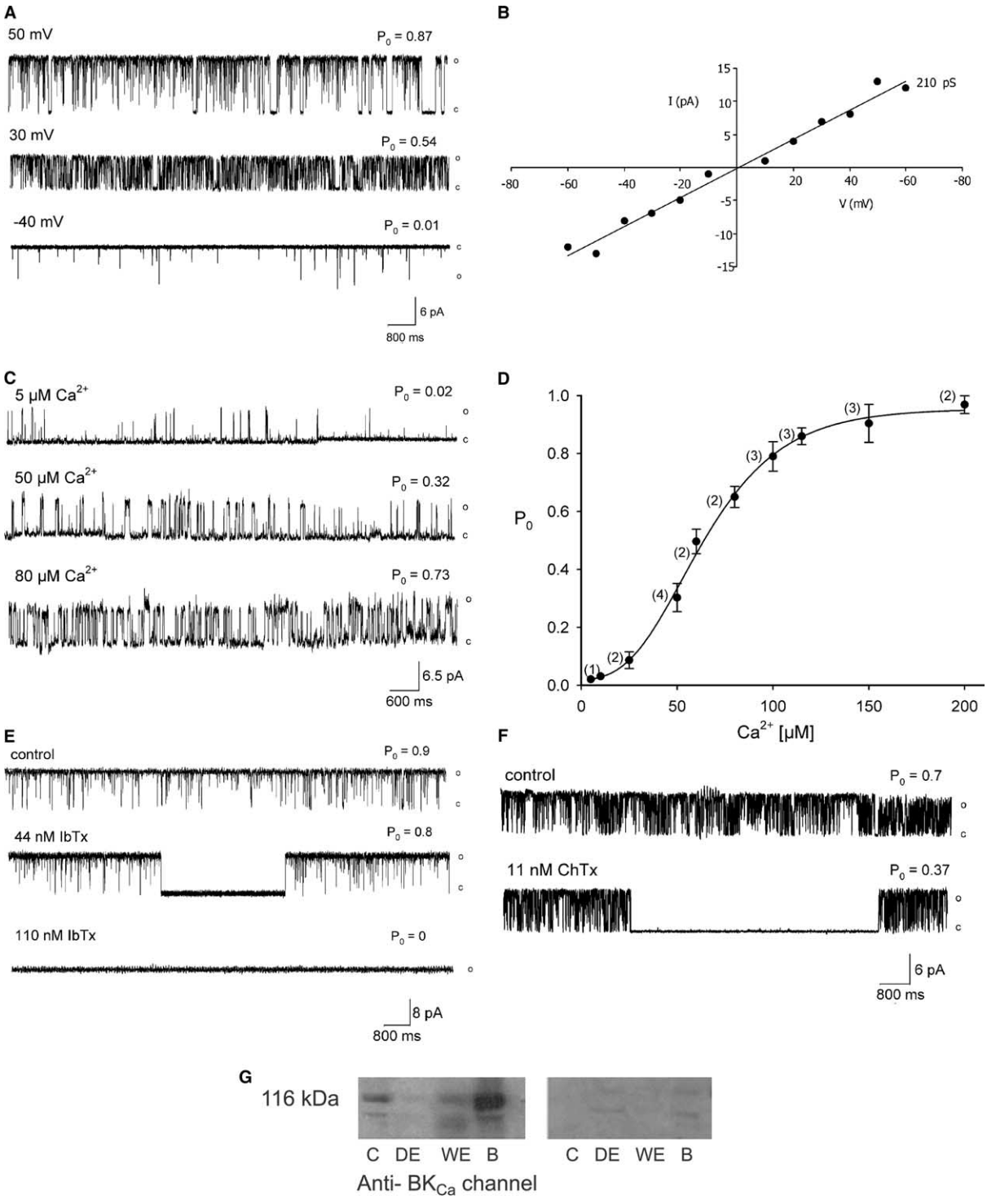

Fig. 5. BK_{Ca} channel. (A) Unitary current recordings of the BK_{Ca} channel from the olfactory ciliary fraction, at three different voltages and 50 μM Ca^{2+}. (B) Representative *I–V* curve, yielding a slope conductance of 210 pS. (C) Unitary current of the BK_{Ca} channel recorded at three different Ca^{2+} concentrations, at 40 mV. (D) P_0 versus $[Ca^{2+}]$ plot of the channel at +40 mV, with the experimental points fitted to a Hill equation, where $K_{0.5}$ = 63.2 μM and n = 2.8. (E,F) Effects of 44 and 110 nM IbTx and 11 nM ChTx on the BK_{Ca} channel, recorded at 50 μM Ca^{2+} and +40 mV. All recordings were obtained in symmetrical 100 mM KAc. (G) Detection of the BK_{Ca} channel by Western blot, using an anti-BK_{Ca} channel (1:500) antibody. A rat brain fraction was used as positive control. A control with the antibody previously adsorbed with antigen is shown at the right-hand side. All lanes were loaded with 50 μg protein.

the effects of pharmacological agents and specific toxins, key tools for ion channel characterization, could not be used in that study for the technical reasons aforementioned. In this study, we circumvented these difficulties by incorporating channels from a purified ciliary membrane fraction into planar lipid bilayers. This allowed the application of phar-

Table 1
Summary of properties of K_{Ca} channels from olfactory cilia membranes

	SK_{Ca}	IK_{Ca}-1	IK_{Ca}-2	BK_{Ca}
Conductance	16 pS	30 and 50 pS	60 pS	210 pS
$K_{0.5}$ for Ca^{2+}	39.8 μM	59.5 μM	ND	63.2 μM
Voltage dependence	No	No	No	Yes
Blocked by	Apamin	Clotrimazole	Clotrimazole	ChTx and IbTx

ND, not determined.

macological agents and toxins from either side of the membrane.

Since our study required a highly purified membrane fraction, we optimized a membrane preparation procedure that involved mechanical rupture of the epithelia and a subsequent series of centrifugation steps of the membrane fraction containing the olfactory cilia [11]. To test the purity of the ciliary membrane preparation, we conducted Western blot analysis with antibodies specific to ciliary membrane proteins, such as ACIII and the CNG channel, and to extra-ciliary membrane proteins, such as the voltage-dependent Na^+ channel. Within the resolution limit of this method, the ciliary membrane fraction exhibited no signs of contamination by other membranes.

Fusion of purified rat olfactory cilia membranes to planar lipid bilayers resulted in the incorporation of small, intermediate and high conductance K_{Ca} channels. From 108 successful channel incorporations, 55%, corresponded to BK_{Ca} channels, 21% to SK_{Ca} channels, 15% to IK_{Ca}-1 channels and 9% to IK_{Ca}-2 channels. These channels shared close similarities regarding conductance and gating kinetics to those recorded with the patch-clamp method in toad olfactory cilia [4]. Considering that the channels originate from different species, the evidence is indicative that channels observed with both methods are virtually identical. A previous study, where odor-triggered whole cell K_{Ca} current properties from the same species were compared, arrived to the same conclusion [21]. Table 1 summarizes the main properties of the K_{Ca} channels identified and characterized in bilayers.

The ~16 pS K_{Ca} channel identified in the present study was voltage-independent and apamin-sensitive, indicating that it belongs to the small-conductance Ca^{2+}-activated K^+ channel family. These K^+ channels typically display 9–20 pS conductances, high K^+ selectivity, activation by Ca^{2+}, voltage-independence and sensitivity to the bee toxin, apamin [22–24]. At least three closely related genes, SK1, SK2, and SK3, encode for SK_{Ca} channel subtypes that share a high structural homology [23]. The SK_{Ca} channel we characterized electrophysiologically probably corresponds to the SK3 identified in the olfactory cilia fraction by Western blot analysis, since it is blocked by apamin in the low nM range [25]. This SK_{Ca} channel displayed a conductance (16 pS) slightly higher than that recorded in toad by patch clamp (10–14 pS; [4]). However, both were voltage-independent and presented similar Ca^{2+}-sensitivities. Interestingly, olfactory cilia SK_{Ca} channels displayed a much lower Ca^{2+} sensitivitiy ($K_d \sim 40$ μM) than the SK1, SK2, or SK3 channels reported in the literature ($K_d \sim 0.3-0.7$ μM) [23].

The IK_{Ca} channel subfamily exhibits a wide range of unitary conductances, from 20 to 80 pS, are insensitive to apamine and some of them are blocked by clotrimazole and ChTx [14,26–28]. We found two IK_{Ca} channels in the bilayers: IK_{Ca}-1, with two open conductance states of 30 and 50 pS, and IK_{Ca}-2, presenting a single 60 pS conductance state. Both channels closely resemble the IK_{Ca} channels recorded by Delgado et al. [4] in toad olfactory cilia, regarding unitary conductances (one of 27 and 58 pS, the other of 60 pS) and kinetics. IK_{Ca}-1 exhibited a $K_{0.5}$ for Ca^{2+} virtually identical to that found by Delgado et al [4]. With regards to IK_{Ca}-2, we could not collect enough data here to obtain its $K_{0.5}$, however, based on its similarity to the equivalent IK_{Ca} recorded with patch clamp [4], it seems likely that it has a similar Ca^{2+}-sentitivity. Furthermore, its CLT-sensitivity supports the view that this channel belongs to the IK_{Ca} family [27].

The 210 pS BK_{Ca} channel exhibited the biophysical characteristics of BK_{Ca} channels from other tissues [14], and was also blocked by ChTx and IbTx. Western blotting confirmed the presence of this channel in the ciliary fraction. It most likely corresponds to the 210 pS BK_{Ca} reported by Delgado et al [4], due to similarities in conductance, voltage dependence and calcium sensitivity ($K_{0.5}$ 63 and 69 μM, respectively). It is also similar to the 240 pS, ChTx-sensitive BK_{Ca} channel described by Jorquera et al. [20] in the toad olfactory cilia fraction. However, BK_{Ca} channels recorded in bilayers [20, and this work] exhibited a maximal P_0 of ~ 1.0, whereas in excised patches it reached a maximal value of ~ 0.4.

One feature of olfactory cilia K_{Ca} channels [this work, 4,20,29] is that they present $K_{0.5}$ in the low micromolar Ca^{2+} range, which is higher that those generally reported in the literature for small, intermediate and high conductance K_{Ca} channels [28,30].

These results and those of Delgado et al. [4] confirm the presence of different K_{Ca} channels in olfactory cilia and support the notion that they might be involved in vertebrate odor-transduction. Although these findings do not allow determining the relative contribution of each K_{Ca} channel subtype to the net ciliary odor-triggered K_{Ca} current, the knowledge of their pharmacology represents an important tool for assessing this problem. For example, the finding that the K_{Ca} current was partially blocked by ChTx and IbTx [10, Madrid et al., unpublished results] indicates a contribution of BK_{Ca} channels to this current. On the other hand, the recent finding that the IK_{Ca}-1 channel could be activated by odor stimulation in oncilium patch-clamp recordings [29], strongly supports the involvement of this K_{Ca} channel in chemotransduction.

Acknowledgments: We are indebted to Ricardo Delgado and Cecilia Vergara for useful discussions and comments on an earlier version of the manuscript. Supported by MIDEPLAN ICM P99-031-F and FONDECYT 1020994.

References

[1] Nakamura, T. and Gold, G.H. (1987) A cyclic nucleotide-gated conductance in olfactory receptor cilia. Nature 325, 442–444.
[2] Kleene, S.J. and Gasteland, R.C. (1991) Calcium-activated chloride conductance in frog olfactory cilia. J. Neurosci. 11, 3624–3629.
[3] Morales, B., Ugarte, G., Labarca, P. and Bacigalupo, J. (1994) Inhibitory K^+ current activated by odorants in toad olfactory neurons. Proc. R. Soc. Lond. B. Biol. Sci. 257, 235–242.
[4] Delgado, R., Saavedra, M.V., Schmachtenberg, O., Sierralta, J. and Bacigalupo, J. (2003) Presence of Ca^{2+}-dependent K^+ channels in chemosensory cilia support a role in odor transduction. J. Neurophysiol. 90, 2022–2028.

[5] Schild, D. and Restrepo, D. (1998) Transduction mechanisms in vertebrate olfactory receptor cells. Physiol. Rev. 78, 429–466.
[6] Dahllan, R.S., Yau, K.-W., Schrader, K.A. and Reed, R.R. (1990) Primary structure and functional expression of a cyclic nucleotide-activated channel from olfactory neurons. Nature (London) 347, 184–187.
[7] Bradley, J., Li, J., Davidson, N., Lester, H.A. and Zinn, K. (1994) Heteromeric olfactory cyclic nucleotide-gated channels: a subunit that confers increased sensitivity to cAMP. Proc. Natl. Acad. Sci. USA 91, 8890–8894.
[8] Leinders-Zufall, T., Greer, C.A., Shepherd, G.M. and Zufall, F.F. (1998) Imaging odor-induced calcium transients in single olfactory cilia: specificity of activation and role in transduction. J. Neurosci. 18, 5630–5639.
[9] Larsson, H.P., Kleene, S.J. and Lecar, H. (1997) Noise analysis of ion channels in non-space-clamped cables: estimates of channel parameters in olfactory cilia. Biophys. J. 72, 1193–1203.
[10] Morales, B., Labarca, P. and Bacigalupo, J. (1995) Inhibitory K^+ current activated by odorants in toad olfactory neurons. FEBS Lett. 359, 41–44.
[11] Washburn, K.B., Turne, T.J. and Talamo, B.R. (2002) Comparison of mechanical agitation and calcium shock methods for preparation of a membrane fraction enriched in olfactory cilia. Chem. Senses 27, 635–642.
[12] Hartree, E.F. (1972) Determination of protein: a modification of the Lowry method that gives a linear photometric response. Anal. Biochem. 48, 422–427.
[13] Morera, F.J., Wolff, D. and Vergara, C. (2003) External copper inhibits the activity of the large-conductance calcium- and voltage-sensitive potassium channel from skeletal muscle. J. Membrane Biol. 192, 65–72.
[14] Vergara, C., Latorre, R., Marrion, N.V. and Adelman, J.P. (1998) Calcium-activated potassium channels. Curr. Opin. Neurobiol. 8, 321–329.
[15] Ramirez, B.U., Behrens, M.I. and Vergara, C. (1996) Neural control of the expression of a Ca^{2+}-activated K^+ channel involved in the induction of myotonic-like characteristics. Cell Mol. Neurobiol. 16, 39–49.
[16] Dionne, V.E. (1992) Chemosensory responses in isolated receptor neurons from *Necturus maculosus*. J. Gen. Physiol. 99, 45–433.
[17] Kang, J. and Caprio, J. (1995) In vivo responses of single olfactory receptor neurons in the channel catfish, *Ictalurus punctatus*. J. Neurophysiol. 73, 172–177.
[18] Morales, B., Madrid, R. and Bacigalupo, J. (1997) Calcium mediates the activation of the inhibitory current induced by odorants in toad olfactory receptor neurons. FEBS Lett. 402, 259–264.
[19] Maue, R.A. and Dionne, V.E. (1987) Calcium mediates the activation of the inhibitory current induced by odorants in toad olfactory receptor neurons. J. Gen. Physiol. 90, 95–125.
[20] Jorquera, O., Latorre, R. and Labarca, P. (1995) Ion channel classes in purified olfactory cilia membranes: planar lipid bilayer studies. Am. J. Physiol. Cell. Physiol. 269, C1235–C1244.
[21] Sanhueza, M., Schmachtenberg, O. and Bacigalupo, J. (2000) Excitation, inhibition and suppression by odors in isolated toad and rat olfactory receptor neurons. Am. J. Physiol. Cell Physiol. 279, C31–C39.
[22] Blatz, A.L. and Maglevy, K.L. (1986) Single apamin-blocked Ca^{2+}-activated K^+ channels of small conductance in cultured rat skeletal muscle. Nature 323, 718–720.
[23] Bond, C.T., Maylie, J. and Adelman, J.P. (1999) Small-conductance calcium-activated potassium channels. Ann. N.Y. Acad. Sci. 868, 370–378.
[24] Stocker, M. (2004) Ca^{2+}-activated K^+ channels: Molecular determinants and function of the SK family. Nature Rev. Neurosc. 5, 758–770.
[25] Grunnet, M., Jensen, B.S., Olesen, S.P. and Klaerke, D.A. (2001) Apamin interacts with all subtypes of cloned small-conductance Ca^{2+}-activated K^+ channels. Pflügers Arch. Euro. J. Physiol. 441, 544–550.
[26] Wolff, D., Cecchi, X., Spalvins, A. and Canessa, M. (1988) Charybdotoxin blocks with high affinity the Ca-activated K+ channel of Hb A and Hb S red cells: individual differences in the number of channels. J. Membrane Biol. 106, 243–252.
[27] Malik-Hall, M., Ganellin, C.R., Galanakis, D. and Jenkinson, D.H. (2000) Compounds that block both intermediate-conductance (IK(Ca)) and small-conductance (SK(Ca)) calcium-activated potassium channels. Brit. J. Pharmac. 29, 1431–1438.
[28] Maher, A.D. and Kuchel, P.W. (2003) The Gardos channel: a review of the Ca^{2+}-activated K^+ channel in human erythrocytes. Internat. J. Biochem. Cell Biol. 35, 1182–1197.
[29] Delgado, R. and Bacigalupo, J. (2004) Cilium-attached and excised patch-clamp recordings of odourant-activated Ca-dependent K channels from chemosensory cilia of olfactory receptor neurons. Europ. J. Neurosci. 20, 2975–2980.
[30] Weiger, T.M., Hermann, A. and Levitan, I.B. (2002) Modulation of calcium-activated potassium channels. J. Comp. Physiol. 188, 79–87.